

The Effect of Different Attenuation Models on the Performance of Routing in Shallow-Water Networks

Giovanni Toso*, Paolo Casari*[‡], Michele Zorzi*[‡]

*Department of Information Engineering, University of Padova, via Gradenigo 6/B, I-35131 Padova, Italy

[‡]Consorzio Ferrara Ricerche, via Saragat 1, I-44122 Ferrara, Italy

E-mail: {tosogiov, casarip, zorzi}@dei.unipd.it

Abstract—Several models can be used to determine the attenuation incurred by sound waves as they travel under water. A trade-off between accuracy and complexity is observed in this respect: the most accurate results are typically yielded by some form of numerical solution to the sound propagation equations, but at the price of high complexity; conversely, simple link budget equations are typically valid only as a first-order approximation, but are much simpler to evaluate. When such different models are applied to network simulations, both the accuracy and the complexity of the chosen model can have a big impact on the simulation time and on the significance of the outcomes.

In this paper, we present a comparison among different models of increasing computational complexity for simulating the transmission loss of underwater acoustic channels, when applied to the simulation of multi-hop underwater acoustic networks. All models have been integrated in the DESERT Underwater framework, which is based on the ns2/MIRACLE network simulator. Our results show that the model and its parameters have in fact a big impact on network simulation results in different network topologies, which is consistent with the findings reported by some other papers that recently appeared in the open literature. Our results also show that in some instances simple propagation models provide a useful approximation if their parameters are properly chosen.

I. INTRODUCTION AND RELATED WORK

In the process of simulating underwater acoustic networks, the attenuation¹ model employed represents a key choice. In fact, the attenuation, as well as its variations over time and space, affect not only the power received over the link between a node and its intended transmitter, but also the impact of interference from concurrent transmissions. Typically, the choice of the attenuation model is driven by the trade-off between the complexity and the accuracy of the model itself. For example, attenuation models in many cases take the form of link budget equations. Such models, as is the case for the propagation loss model taken from [1] and effectively redrawn in the scope of underwater communications in [2], are very simple to evaluate, but practically oblivious both to boundary conditions (such as the physical parameters of the water and the shape of the sea surface and bottom) and to channel response changes over time (e.g., due to the time variations of such environmental parameters). Other models such as [3] apply numerical methods

The authors would like to thank the Woods Hole Oceanographic Institution, Dr. James Preisig, the SPACE08 and the KAM11 research personnel for making the experimental data sets available. This work has been partially supported by the US Office of Naval Research under Grant no. N62909-14-1-N127.

¹In this paper we refer to attenuation as the inverse of the channel power gain, and to absorption as the conversion of compressional wave energy into heat.

to solve the propagation equations for sound in bounded layered media: this yields a more accurate representation of the sound field, though at the price of higher complexity. In addition, such complexity has to be paid every time environmental parameters change, and the numerical process has to be re-run. Intermediate solutions also exist: for example, the model adopted in [4] takes into account an approximation of the environmental conditions, but still relies on simple equations to compute the attenuation; the authors in [5] show that there is agreement between a network performance model based on stochastic geometry and Bellhop simulations, provided that the spreading factor of the model in [2] is appropriately fitted to match the average channel power gain computed by Bellhop; the authors in [6] introduce the Mime channel simulator, which emulates (either directly or statistically) the delay and Doppler spread of channels measured during at-sea experiments.

Primed by [1], [2], many works on underwater networking have computed attenuation as the superposition of a spreading loss and an absorption loss, where the latter is a frequency-dependent term usually modeled via Thorp's equation [2]. A first attempt to move beyond this model (while accepting greater physical layer simulation complexity) came in [7], where the authors simulate the sound propagation via the Bellhop ray tracing software, for the case where all environmental parameters are fixed a priori. The work in [8] extends this approach via a flexible framework named WOSS, where the users configure basic network parameters (e.g., the geographical locations of the nodes) and WOSS automatically retrieves environmental parameters from oceanographic databases and feeds them to Bellhop, from which it retrieves the channel power gains required for the network simulation.

Other papers took a system-level approach, based on modeling either the underwater channel statistics under some simplifying assumption [9] or directly the error rate of packets transmitted according to a given modulation scheme in specific environmental conditions [10]. The main shortcoming of these models is that they can only reproduce accurately the same environmental conditions and physical layer configuration over which the statistical models were trained.

The inclusion of more precise state equations to relate the speed of sound to the physical characteristics of the water, and thereby infer the propagation delay (as opposed to setting a fixed propagation speed of about 1500 m/s), is discussed in [11]. The work in [4] considers a model due to Rogers which, unlike the model in [1], considers an approximation of the

sound speed profile (SSP) in shallow waters (namely, a negative sound speed gradient with increasing depth) and accounts for power losses affecting the components of the sound field that bounce off the bottom one or multiple times. The same model is shown in [4] to provide a better accordance between simulations and at-sea experiments in shallow water scenarios.

In this work we evaluate the impact of the Urick and Rogers attenuation models on the performance of multihop routing in underwater networks (in terms of packet delivery ratio), and compare the results to what would be predicted by simulating realistic attenuation via the Bellhop ray tracing software. The analysis includes three network scenarios involving increasing levels of interference. Our results show that while the Bellhop and Rogers models are expected to yield reasonably realistic results [4], [8], the Urick model can still work as a sufficiently accurate approximation, provided that the spreading exponent is appropriately chosen.

II. ATTENUATION MODELS

A. “Urick” model

This model was first employed in [2] for the analysis of the Signal-to-Noise Ratio (SNR) and capacity of underwater acoustic links. It is based on empirical equations for acoustic power spreading and absorption losses. In the absence of mobility, the model yields a time-invariant output. The attenuation incurred by a signal transmitted at a frequency f (in kHz) over a distance d (in m) is given by [2, Eq. (2)]:²

$$10 \log_{10} A(d, f) = k \cdot 10 \log_{10} d + d \cdot \alpha(f), \quad (1)$$

where d is the source-receiver distance, k is the spreading exponent ($k = 1$ corresponds to cylindrical spreading, $k = 2$ to perfectly spherical spreading) and $\alpha(f)$ is the absorption loss in dB/m. Using Thorp’s equation, for $f > 0.4$ kHz (as is the case in this paper) we have

$$\alpha(f) = \frac{1}{914.4} \left(\frac{0.11 f^2}{1 + f^2} + \frac{44 f^2}{4100 + f^2} + 2.75 \cdot 10^{-4} f^2 + 0.003 \right) \quad (2)$$

B. “Rogers” model

In [14], Rogers presented a model to predict acoustic attenuation in shallow water subject to mode stripping and cylindrical propagation. The following attenuation formula (3) is valid when the effective angle of the last mode stripped $\theta_g \geq \theta_L = \max\{\theta_g^{\max}, \theta_C\}$ where θ_g^{\max} is the maximum grazing angle for a Refracted-Bottom-Reflected (RBR) mode and θ_C is the cutoff angle of the lowest mode:

$$A(d, f) = 15 \log_{10} d + 5 \log_{10}(h\beta) + \frac{\beta d \theta_L^2}{4h} - 7.18 + \alpha(f)d. \quad (3)$$

Otherwise, when $\theta_g < \theta_L$, (4) must be used:

$$A(d, f) = 10 \log_{10} d + 10 \log_{10} \left(\frac{h}{2\theta_L} \right) + \frac{\beta d \theta_L^2}{4h} + \alpha(f)d, \quad (4)$$

²We remark that (1) is dimensionally correct only if $k = 2$. However, even when $k < 2$, it is always possible to insert a term that makes the equation dimensionally correct (as in (3) and (4), discussed later). In Section III, we will show that this approach works as an approximation to model otherwise complex scenarios. This procedure is common in radio propagation modeling [12], [13].

where d is the transmitter-receiver range (in m), h is the uniform height of the water column (in m), β is the bottom loss coefficient (in dB/rad) determined from the Rayleigh reflection coefficient, and $\alpha(f)$ is Thorp’s absorption loss factor. The computation of the coefficient β depends on several values like the water and bottom sediment density and the sound speed of sound in water and in the sediment.

C. Bellhop

The Bellhop software [3] exploits ray tracing to predict, among other things, the attenuation incurred by a signal traveling in an underwater channel, given the geometry of the environment (e.g., surface shape, bottom shape, position of transmitter and receiver) and its physical characteristics (e.g., SSP, bottom sediments). In this work, we employed Bellhop as a more accurate, yet more numerically complex alternative to the empirical attenuation models summarized in Sections II-A and II-B. The next section briefly describes our simulation environment and explains how the Urick, Rogers and Bellhop models have been integrated in our simulation framework.

III. RESULTS

A. Simulation framework

All simulations presented in this section have been carried out with the ns2/MIRACLE-based DESERT Underwater framework [15]. The Urick model is natively implemented in DESERT. The Rogers model has been integrated as a new propagation model. Among other inputs, this model requires the specification of the sound speed at the surface and at the bottom of the transmission scenario. We chose to employ the SSPs measured during the KAM11 experiment [16] and employed in our previous study [17]³. From the dataset, we extract one SSP measurement every 30 s, and feed the surface and bottom samples to the Rogers model. Furthermore, we assume fine-grained sandy bottom sediments.⁴ The same SSP and environmental parameters are fed to Bellhop to predict time-varying attenuation patterns. In this case, we assumed flat surface and bottom, and discretized the source and receiver depth from 5 to 95 m in steps of 5 m, and the receiver range from 50 m to 10 km in steps of 50 m. The attenuation information derived via either model is employed to compute the attenuation incurred both by the desired signal and by interference. For the Urick and Rogers models, the one-way propagation delay is set according to the value of the sound speed at the surface; for Bellhop, such delay equals the time of flight of the first arrival. In all cases, the noise model is simulated via the empirical equations in [2, Eq. (6)], where we set the shipping factor to 0.5 and the wind speed to 0 m/s.

B. Scenario

We consider three multihop network topologies labeled linear, star and parallel, respectively depicted in Figs. 1, 2 and 3.

³A graphical representation of the SSPs is available in [17, Fig. 3].

⁴The relative attenuation coefficient of the sediment is 0.51, the density of the sediment is 1.941 g/cm³ and the sound speed in the sediment is 1650 m/s as reported in [14].

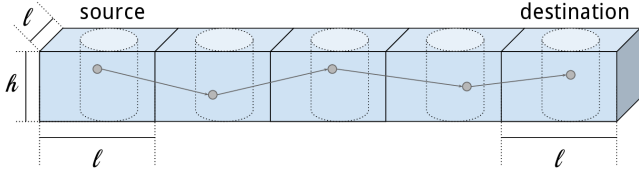


Fig. 1. Linear topology.

Each topology is drawn around a number of cells of depth $h = 100$ m and given side d . In each cell, a node is placed at random within a cylinder of height h and base diameter equal to $\min\{\ell/2, 200$ m $\}$.

The performance of the physical layer is modeled according to the Binary Phase Shift Keying (BPSK) error equations,⁵ assuming independent bit errors across a packet and modeling interference as a time-varying Gaussian contribution to the Signal-to-Interference and Noise Ratio from which the bit error probability is computed. The system has a bandwidth of 16 kHz and a carrier frequency of 26 kHz. The bit rate is 2000 bit/s and the Source Level is set to 138 dB re μPa^2 relative to a distance of 1 m from the source. The parameters have been chosen to mimic the specifications of the S2CR 18/34 WiSE Underwater Acoustic Modem manufactured by EvoLogics GmbH as described in [18], [19]. A 1-persistent Carrier Sense Multiple Access (CSMA) protocol is used at the MAC layer as in [17]. In the parallel and star topologies, instead, there are two sources (labeled 1 and 2) that transmit their generated packets to their respective destination (also labeled 1 and 2) on the opposite side of the network. To do so, a static routing protocol with a pre-determined route that traverses all cells connecting the source to the destination is employed. For example, if we number the relays between the source and the destination in the linear topology (Fig. 1) as R1, R2 and R3, the static route employed here is source \rightarrow R1 \rightarrow R2 \rightarrow R3 \rightarrow destination. Hence, each packet correctly delivered to the destination travels exactly 4 hops in all cases. Data packets are generated periodically at a rate of 1 packet every 30 s. This is nominally enough for a packet to traverse a route and be delivered before a new one is generated. In the presence of 2 sources, the packet generation processes are synchronous. This choice aims at measuring the impact of interference from concurrent transmissions on the performance of multihop routing. In this perspective, the linear, star and parallel topologies imply progressively higher levels of interference. All packets are 125 bytes long, corresponding to a packet transmission time of 0.5 s. No retransmissions are performed in case of errors. The simulation time is set to about 8 hours, so that one day of SSP measurements from the KAM11 experiment is covered. The data packet generation process is stopped 10 min before the end of the simulation, to allow the delivery of all packets that may have remained in the queue of the nodes. Each point in the plots is obtained by averaging the output of 100 simulation runs, where the node locations are re-drawn before each run.

⁵For Bellhop, this corresponds to computing the received power from the coherent sum of all arrivals.

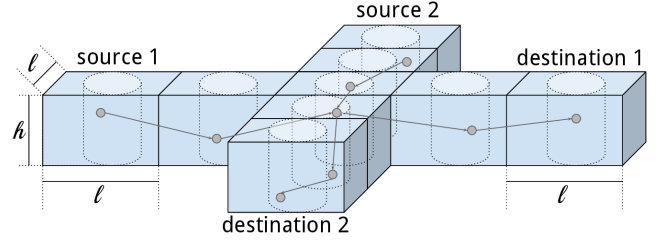


Fig. 2. Star topology.

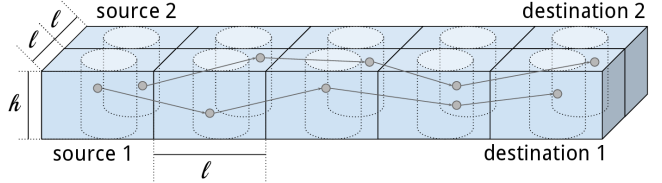


Fig. 3. Parallel topology.

C. Simulation results

In this section we present the results of the simulation campaign. In Figures 4, 5 and 6 we show, for each topology, the Packet Delivery Ratio (PDR) as a function of the cell side length ℓ .⁶ The figures contain one curve for the Bellhop and Rogers model, and a set of curves for the Urick model, each corresponding to a different value of the spreading exponent k in (1). This corresponds to an interpretation of (1) as a model with one parameter to be fitted, from 1.5 up to 1.75.

We start from the simplest linear network case (Fig. 4), where no interference is expected and the cell side ℓ is the only key factor for the network performance. For $\ell \leq 1300$ m the PDR is always very close to 1 for all models. In this configuration, the cell side is sufficiently short to yield a limited attenuation, which allows all nodes to forward packets correctly to their next hop, up to the destination. Starting from $\ell = 1400$ m, the attenuation is sufficient to start causing errors. The PDR for the Rogers model case decreases slightly before the PDR in the Bellhop case for increasing ℓ . Among the several spreading exponents considered for Urick's models, we observe that $k = 1.75$ and $k = 1.7$ fit well the behavior of the Rogers and Bellhop models, respectively. The latter is in line with the findings and conclusions in [5]. As expected from (1), the PDR, for increasing ℓ , is higher for curves related to lower values of k . For example, in the case $k = 1.5$, which is used in a large portion of the literature relying on the Urick model to compute attenuation, it is still possible to send some data correctly through the network up to $\ell = 2500$ m, i.e., 500 m longer than predicted by Bellhop.

In the star topology network (Fig. 5), the node placed in the middle contributes actively to two source-destination flows. In this case, even for large values of the cell side, one node will be shared between the two paths. For this topology we expect some interference concentrated around the area where the shared node is located. We recall that the packet generation

⁶Assuming that two nodes are placed at the center of two contiguous cells, and that $500 \text{ m} \leq \ell \leq 3000$ m, the nodes experience an SNR ranging in [21.7, 33.4] dB for $k = 1.5$ and in [13.0, 26.7] dB for $k = 1.75$ (in the absence of interference).

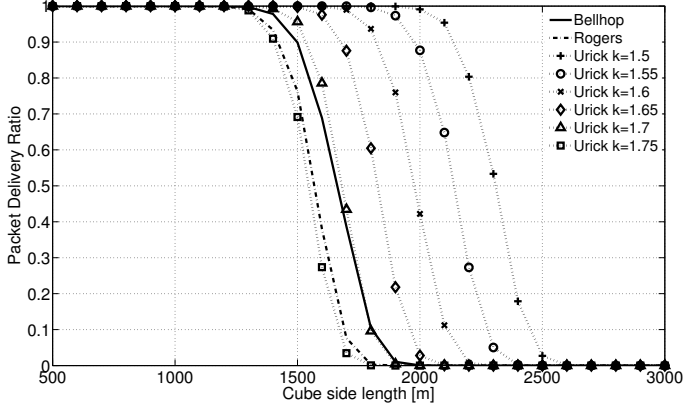


Fig. 4. Packet delivery Ratio in the Linear topology.

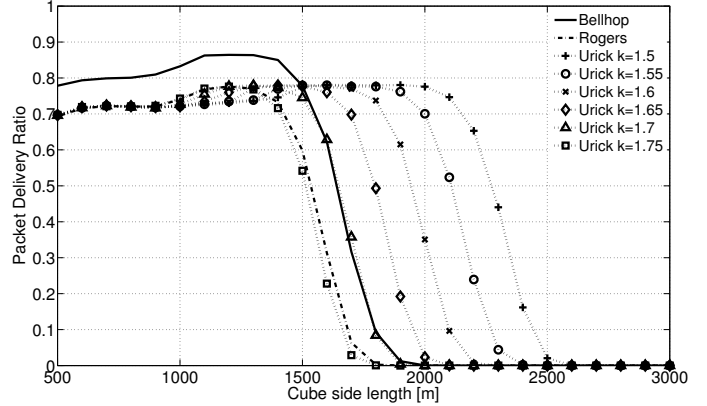


Fig. 5. Packet Delivery Ratio in the Star topology.

processes are synchronous, hence each route is expected to convey packets to the middle node almost at the same time (where small displacements are expected due to the random location of each node within its own cell). In any event, the packets from source 1 and source 2 are expected to interfere in correspondence of their second hop. Due to this, for $\ell \leq 1000$ m the PDR for the Urick and Rogers curves is similar and roughly equal to 0.7. We note that it does not decrease to 0, mostly due to a non-zero chance of capturing one of the two packets at the middle node. For larger values of ℓ , the PDR increases up to 0.8, and decreases after that. In fact, increasing ℓ reduces the impact of interference, but tends to make the network noise limited when ℓ is large. This is also in accordance with the observations in [5]. Again, the Rogers curve corresponds roughly to the Urick curve for $k = 1.75$ and, with the exception of the region $\ell \leq 1700$ m, the Bellhop curve is well approximated by the Urick curve for $k = 1.7$. The discrepancy is caused by the more accurate prediction of the sound field interference patterns performed by Bellhop, which translates into a lower average amount of interference due to concurrent transmissions. In any event, the Urick curve for $k = 1.7$ has the same behavior as the Bellhop curve (initial increase, then decrease after $\ell = 1500$ m). This confirms that the Urick model is a valid first-order approximation, provided that k is appropriately chosen to fit the results.

In the parallel topology the position of the nodes leads to a larger amount of interference with respect to the star topology, as each transmission from a relay in a route will interfere with the one from the corresponding relay in the other path. In this topology, the Urick and Rogers models (Fig. 6) return similar performance up to $\ell = 800$ m where the PDR is about 0.6 (which is expectedly lower than in the star topology case). For increasing values of ℓ , the PDR increases (where the maximum value depends on k). We remark that a low value of k increases the resistance of the signal to noise, but makes interference stronger. For example, for $k = 1.5$ the PDR curve starts decreasing (noise-limited regime) for $\ell > 2000$ m. However, for lower values of ℓ (interference-limited regime) the same curve increases significantly only for $\ell > 1200$ m. Conversely,

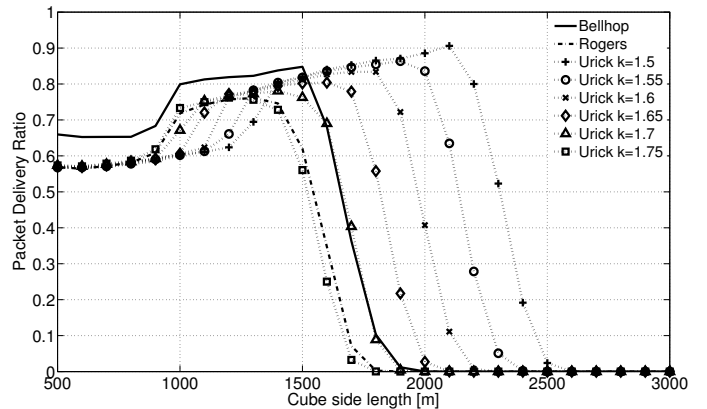


Fig. 6. Packet delivery Ratio in the Parallel topology.

higher values of k , e.g., $k = 1.75$, lead to higher attenuation: in turn, this reduces the impact of interference (the PDR curve increases starting from $\ell > 900$ m), but makes signals more prone to noise (the PDR decreases already for $d \approx 1300$ m). Again, the Rogers model curve behaves similarly to the Urick model curve with $k = 1.75$ and the Bellhop curve corresponds well to the Urick curve for $k = 1.7$.

IV. CONCLUSIONS

In this paper we presented a comparison among different models for simulating the signal attenuation over underwater acoustic channels. We considered three models, and evaluated their impact on the PDR of a static routing protocol in three different topologies. We showed that the choice of a given model (and the parameters thereof) can have a big impact on the estimated network performance. Moreover, we showed that the Rogers and Bellhop models, which have been shown to provide realistic results in the literature with respect to the Urick model, can still be approximated well by the latter by tuning the spreading loss exponent, and that the value that achieves the match is the same across all topologies, despite their being subject to different amounts of interference. This result means that the Urick model (which is simple and fast to evaluate) can be used as a computationally fast first-order approximation for the attenuation in multihop underwater networks.

REFERENCES

- [1] R. Urick, *Principles of Underwater Sound*. New York: McGraw-Hill, 1983.
- [2] M. Stojanovic, "On the relationship between capacity and distance in an underwater acoustic communication channel," *ACM Mobile Comput. and Commun. Review*, vol. 11, no. 4, pp. 34–43, Oct. 2007.
- [3] M. Porter *et al.*, "Bellhop code." [Online]. Available: <http://oalib.hlsresearch.com/Rays/index.html>
- [4] M. Zuba, Z. Jiang, T. Yang, Y. Su, and J. Cui, "An advanced channel framework for improved underwater acoustic network simulations," in *Proc. IEEE/MTS OCEANS*, San Diego, CA, Sep. 2013.
- [5] K. Stamatiou, P. Casari, and M. Zorzi, "The throughput of underwater networks: Analysis and validation using a ray tracing simulator," *IEEE Trans. Wireless Commun.*, vol. 12, no. 3, pp. 1108–1117, Mar. 2013.
- [6] R. Otnes, P. van Walree, and T. Jensenrud, "Validation of replay-based underwater acoustic communication channel simulation," *IEEE J. Ocean. Eng.*, vol. 38, no. 4, pp. 689–700, Oct. 2013.
- [7] N. Parrish, L. Tracy, S. Roy, P. Arabshahi, and W. Fox, "System design considerations for undersea networks: link and multiple access protocols," *IEEE J. Sel. Areas Commun.*, vol. 26, no. 9, pp. 1720–1730, Dec. 2008.
- [8] F. Guerra, P. Casari, and M. Zorzi, "World Ocean Simulation System (WOSS): a simulation tool for underwater networks with realistic propagation modeling," in *Proc. of ACM WUWNet 2009*, Berkeley, CA, Nov. 2009.
- [9] F. Pignieri, F. De Rango, F. Veltri, and S. Marano, "Markovian approach to model underwater acoustic channel: Techniques comparison," in *Proc. IEEE MILCOM*, San Diego, CA, Nov. 2008.
- [10] B. Tomasi, P. Casari, L. Finesso, G. Zappa, K. McCoy, and M. Zorzi, "On modeling JANUS packet errors over a shallow water acoustic channel using Markov and hidden Markov models," in *Proc. IEEE MILCOM*, San Jose, CA, Oct. 2010.
- [11] A. Sehgal, I. Tumar, and J. Schönwälder, "AquaTools: An underwater acoustic networking simulation toolkit," in *Proc. MTS/IEEE OCEANS*, Sydney, Australia, May 2010.
- [12] H. Lim, L.-C. Kung, J. C. Hou, and H. Luo, "Zero-configuration indoor localization over IEEE 802.11 wireless infrastructure," *Wireless Networks*, vol. 16, no. 2, pp. 405–420, Mar. 2010.
- [13] A. Coluccia, "Reduced-bias ML-based estimators with low complexity for self-calibrating RSS ranging," *IEEE Trans. Wireless Commun.*, vol. 12, no. 3, pp. 1220–1230, Mar. 2013.
- [14] P. H. Rogers, *Onboard Prediction of Propagation Loss in Shallow Water*. Washington, DC: Naval Research Lab Defense Technical Information Center, Washington, DC, 1981.
- [15] R. Masiero, S. Azad, F. Favaro, M. Petrani, G. Toso, F. Guerra, P. Casari, and M. Zorzi, "DESERT Underwater: an NS-Miracle-based framework to DEsign, Simulate, Emulate and Realize Test-beds for Underwater network protocols," in *Proc. IEEE/OES OCEANS*, Yeosu, Republic of Korea, May 2012.
- [16] W. S. Hodgkiss and J. C. Preisig, "Kauai Acomms MURI 2011 (KAM11) experiment," in *Proc. of European Conference on Underwater Acoustics (ECUA)*, Aberdeen, United Kingdom, Jul. 2012.
- [17] B. Tomasi, G. Toso, P. Casari, and M. Zorzi, "Impact of time-varying underwater acoustic channels on the performance of routing protocols," *IEEE J. Ocean. Eng.*, vol. 38, no. 4, pp. 772–784, Oct. 2013.
- [18] "Evologics," Last time accessed: February 2014. [Online]. Available: <http://www.evologics.de/>
- [19] K. G. Kebkal and R. Bannasch, "Sweep-spread carrier for underwater communication over acoustic channels with strong multipath propagation," *The Journal of the Acoustical Society of America*, vol. 112, no. 5, pp. 2043–2052, 2002.